Seismic moment tensor solutions and geophysical settings in the Philippine Sea basin mapped by GMT

Polina Lemenkova

Revista Geofísica • 69 • 2019 • Artículos • 17-34
ISSN (impresa): 0252-9769 • ISSN (en línea): 2663-4015
DOI: https://doi.org/10.35424/rgf.i70.939

Seismic moment tensor solutions and geophysical settings in the Philippine Sea basin mapped by GMT

Soluciones del tensor de momento sísmico y condiciones geofísicas en la cuenca del Mar de Filipinas mapeada con GMT

Polina Lemenkova[1]

Recibido el 14 de julio de 2020; aceptado el 17 de noviembre de 2021

Abstract

The study is focused on mapping geophysical settings on the margins of the Philippine Sea Plate (PSP). Active volcanism and seismic situation along the margins of the Philippine Sea Basin (PSB) shows earthquake events demonstrating high seismicity of the region caused by tectonic plate subduction. The aim was to perform cartographic mapping of the earthquake events using Generic Mapping Tools (GMT) modules, to analyze seismic situation through visualization of the geophysical datasets. The data was processed by GMT using multi-source data: GEBCO, CMT and ISC seismic data. Technically, a set of GMT modules was used ('psmeca', 'psvelo', 'grdtrack', 'grdimage') for data modelling and mapping. An application of GMT functionality is presented by selected code snippets with selected code snippets for 'psmeca' and 'psvelo', 'img2grd', 'img2grd' modules. Current paper presents a report on the cartographic techniques applied for geophysical mapping. Centroid moment tensor solutions are visualized for shallow depth earthquakes of Mw <10 along the PSB margins from 1976 to 2010. Earthquakes along the tectonic plate subduction zone are shown by GMT. Data from Global Centroid-Moment-Tensor (CMT) Project. Presented and explained GMT code snippets contribute to the development of methods in geological mapping using GMT scripting toolset, for visualizing focal mechanisms.

Key words: *Mapping, cartography, GMT, earthquake, geophysics, Philippine Sea, geology*

[1] Schmidt Institute of Physics of the Earth, Russian Academy of Sciences. Department of Natural Disasters, Anthropogenic Hazards and Seismicity of the Earth. Laboratory of Regional Geophysics and Natural Disasters, Russian Federation, e-mail: pauline.lemenkova@gmail.com
ORCID: https://orcid.org/0000-0002-5759-1089

Resumen

El presente studio se enfoca al mapeo geofísico en los límites de la Placa Marina de Filipinas (PSP por sus siglas en inglés). En particular, la actividad volcánica y sísmica en los límites de la Cuenca del Mar de Filipinas (PSB por sus siglas en inglés), es evidente por la gran actividad en la region cuyo origen está relacionado con la subducción de esta placa tectónica. El objetivo consiste en realizar un mapeo cartográfico de los eventos sísmicos utilizando los módulos del programa "Generic Mapping Tools" (GMT), para analizar el estado de la actividad sísmica a través de la visualización de las bases de datos geofísicos. Los datos se procesaron utilizando GMT con el apoyo de diversas bases de datos sismológicos, tales como GEBCO, CMT y ISC. Técnicamente, se utilizaron los módulos de GMT en donde se observa su funcionalidad mediant el apoyo de fragmentos de diversos códigos (tales como 'psmeca', 'psvelo', 'grdtrack', 'grdimage') para el modelado y el despliegue de datos. Se presenta también una aplicación de los módulos de GMT mediante fragmentos de códigos particulares tales como 'psmeca', 'psvelo', 'img2grd', 'img2grd'. El presente artículo representa un informe sobre las técnicas cartográficas aplicadas al mapeo en geofísica. Las soluciones del tensor momento del centroide se visualizan para terremotos de poca profundidad de Mw <10 a lo largo de los márgenes de la PSB entre 1976 y 2010. Se muestran los terremotos a lo largo de la zona de subducción entre las placas tectónicas utilizando GMT utilizando los datos del Proyecto Global Tensor de Momento del Centroide (CMT, por sus siglas en inglés). El uso de fragmentos de código GMT presentados y explicados contribuyen al desarrollo de métodos en mapeo geológico utilizando el conjunto de herramientas de secuencias de comandos GMT, para visualizar mecanismos focales.

Palabras Clave*: Mapeo, cartografía, GMT, terremoto, geofísica, mar de Filipinas, geología.*

1. Introduction

Geomorphological evolution of the oceanic trenches is largely controlled by a variety of factors including geological settings, tectonic plate movements and geomorphological profiling (Fujioka *et al.,* 2002; Gong *et al.*, 2017; Lemenkova, 2018; 2019a; 2019b), geophysical processes (Ogawa *et al.*, 1997; Hall *et al.*, 1995a; Seekings & Teng, 1977), submarine volcanism and slope steepness (Ozawa *et al.*, 2004; Lemenkova, 2019c, 2020f) inducing intensity of sedimentation and marine biological factors contributing to the sediment supply. Earlier studies on oceanic trenches highlighted relationship between the geomorphic patterns of the deep-sea channels, submarine fans and their topography related to the mid-ocean ridge tectonics, volcanism and dynamics of the Philippine back arc (Menard, 1955; Chang *et al.*, 2007; Fujioka *et al.*, 1999, Lemenkova, 2019d; Hall *et al.*, 1995b), as well as earthquakes and gravitation (Lin & Lo, 2013). Double seismic zone beneath the Mariana Island arc is explained (Samowitz & Forsyth, 1981) by the following conceptual scheme of the processes of the global plate tectonics.

Subduction of the cooled plate into the mantle causes formation of the deep ocean trenches where, as a consequence, earthquakes and tsunamis originate.

Active volcanism and seismic situation around Philippine Sea margins (Figure 5) shows earthquake events demonstrating high seismicity of the region caused by tectonic plates subduction. Subducting lithospheric plates act as giant radiators of the heat cooling, thickening, and progressively subsiding from ridge to trench. As a result, spreading seafloor, affected by moving plates, creates an axial rift, corrugated hills, and ridges, formed by the nearby faults.

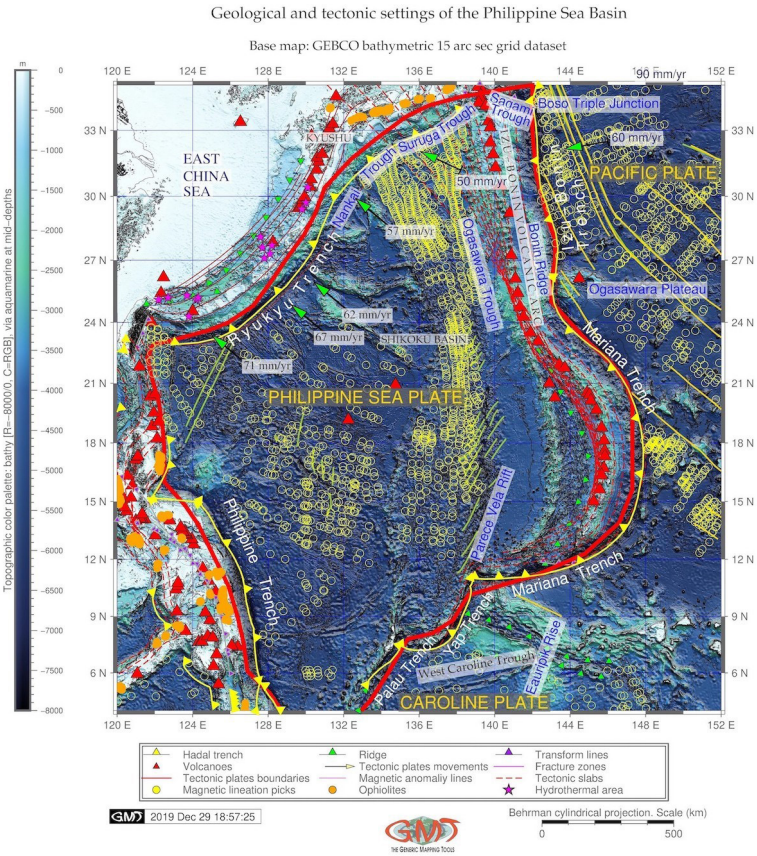

Figure 1. Geologic map of the Philippine Sea Basin. Solid red lines indicate boundaries between the lithospheric plates. Yellow fronts denote trench axes. Tectonic slab contours are depicted by the red dashed lines. Green arrows and relevant numbers indicate the convergence rates (mm/year) along the trenches. Magenta triangles denote hydrothermal areas mostly located along the Ryukyu Trench.

Source: author.

Plate subduction along the Izu-Bonin-Mariana (IBM) trench caused trench roll-back, arc rupture and back-arc rifting of two interconnected back-arc basins: Parece Vela and Shikoku Basins. The KPR, a remnant arc of the active IBM system results from the spreading of the Shikoku Basin (Figure 1). It plays a key role in the subduction process of the west Philippine Sea Plate: the subduction zone here is characterized by the Kyushu-Palau Ridge (KPR) subducting beneath the Kyushu Arc, Figure 1 (Cao *et al.*, 2014). A set of geodynamic processes including subduction-interface rheology, phase-transition buoyancy, slab stagnation, rollback of mantle and ridge-push effects, cause significant trench motion of the IBM detected as advance by global plate-motion observations (Cížková, H., Bina, 2015).

2. Materials and Methods

2.1. Seismic mapping

Focal mechanisms (Figure 2) were drawn using 'psmeca' module of Generic Mapping Tools (GMT) that reads dataset values from ASCII file and generates a PostScript code plotting focal mechanisms. Focal mechanisms depict a commonly accepted theory of the focal depths of the earthquake, showing a depth from the surface to the earthquake's origin (a.k.a. hypocenter). Given dataset contains significant amount of shallow earthquakes of the PSB with focal depths of several tens kilometers (mostly <50), intermediate earthquakes with focal depths from 70 to 200 kilometers, and also a few earthquakes of PSB with deep focus reaching depths >500 kilometers, Table 1. The foci of the most PSB earthquakes are concentrated in the crust and upper mantle, that is, originate in shallow parts of the Earth's interior.

The original dataset of the focal mechanism solutions are from the was taken from the Global CMT Catalog, formerly known as the Harvard CMT catalog (Ekström *et al.*, 2012). Technical parameters are set up as following:

- Moment magnitude (Mw) <10;
- Surface wave magnitude (Ms): <10);
- Body wave magnitude (Mb): <10;
- Data time span: 1976-2010

While magnitude is a widely understood concept, describing the energy of the earthquake release on a logarithmic scale, some technical details are presented in Table 1 and Table 2 used for mapping velocity (Figure 4), assigning and interpreting magnitudes. Introduced in the 1930's, the Richter Scale is the best known scale for measuring the magnitude of earthquakes (Müller, 2001). Surface wave magnitude (Ms), creating the strongest disturbance within the upper layers of the Earth, is computed by the following algebraic formula:

$$MS=\log10(A/T)+1.66\log10(D)+3.30,$$

where *T* is the measured wave period and *D* is the distance in radians.

On the contrary, earthquakes occurring deep in the Earth do not generate large surface waves. Therefore, a body wave magnitude (Mb) is scaled based on the seismic waves penetrating through the Earth's interior (body) (Müller, 2001). Body wave magnitude (mb) is measured based on the maximum amplitude A by formula:

$$Mb=\log10(A/T)+Q(D,h)$$

where *T* is the measured wave period and *Q* is an empirical function of focal depth h and epicentral distance *D*.

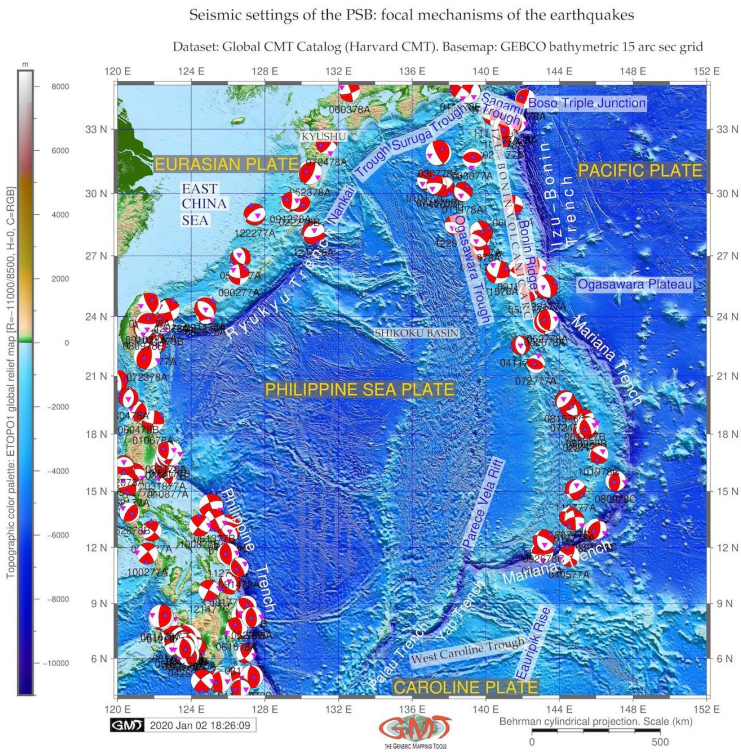

Figure 2. Seismic map of the focal mechanisms: PSB margins. Centroid moment tensor solutions for shallow depth earthquakes of Mw <10 along the PSB margins from 1976 to 2010. Earthquakes along the tectonic plate subduction zone are shown by GMT. Data from Global CMT Project. Source: author.

Table 1. Earthquake events for 1976-1977

Table 1 Earthquake events for 1976/1977

Location code	Date	Centroid Time	Lat (°N)	Lon (°E)	Depth	HD*	CHT**
021576A PHILIPPINE ISL	1976/2/15	1:54:30.3 GMT	13.12	126.02	15.6	4.2	7.2
060776A LUZON PHILIPPINE ISL	1976/6/7	7:36:0.3 GMT	14.23	125.07	24.4	4.8	4.9
081676B LEYTE	1976/8/16	16:11:58.7 GMT	7.07	123.75	33.0	21.7	51.4
081776A LEYTE PHILIPPINE ISL	1976/ 8/17	1:11:16.5 GMT	10.08	126.10	47.3	2.6	6.3
081776B MINDANAO	1976/8/17	4:19:39.8 GMT	7.14	123.01	15.0	8.7	12.5
092976A MINDANAO	1976/9/29	21: 2:31.5 GMT	6.61	124.24	15.0	1.8	-1.2
110776B MINDANAO	1976/11/7	17: 9:13.7 GMT	8.35	126.86	42.1	6.2	7.6
112276A MINDANAO	1976/11/22	4:22:20.7 GMT	7.03	123.58	60.0	3.0	-4.6
121476A RYUKYU ISLANDS	1976/12/14	16: 6:49.2 GMT	28.12	130.64	15.0	3.8	4.8
010177C SOUTH OF HONSHU JAPAN	1977/ 1/1	11:33:45.9 GMT	30.62	136.80	476.5	1.8	4.3
010777B TAIWAN REGION	1977/1/7	19:36:48.6 GMT	20.78	120.01	10.0	2.5	1.7
010877A LUZON PHILIPPINE IS.	1977/1/8	6:41:10.9 GMT	15.77	122.73	13.3	1.6	6.8
011577A PHILIPPINE ISL	1977/1/15	10:49: 8.8 GMT	12.80	126.06	32.9	2.2	3.0
011777A BONIN ISL REGION	1977/1/17	6:23:40.7 GMT	26.40	142.74	13.9	3.4	4.6
011977B MINDANAO	1977/1/19	13:54: 9.8 GMT	5.01	126.56	50.1	4.8	5.3
012077A MINDANAO, PHILIPPINE	1977/1/20	20:51:17.2 GMT	8.00	122.70	41.8	2.3	2.3
022777A MARIANA ISLANDS	1977/ 2/27	18:34:15.0 GMT	18.21	145.30	592.6	2.1	6.5
022877B MINDANAO, PHILIPPINE IS	1977/2/28	1:50:38.7 GMT	8.87	127.01	55.8	2.3	6.8
030277B MINDANAO, PHILIPPINE IS	1977/3/2	9:53:26.4 GMT	6.62	123.53	33.4	6.0	3.2

*Half duration; **Centroid hypocenter time (HT)

Table 2. Magnitude and Moment Tensor

Table 2 Magnitude and Moment Tensor

Location code	Moment Tensor	Mw*	Mb**	Ms***	SM****	FP_1*****	FP_2******
021576A Philippine Isl	Expo=25 -5.140 3.270 1.860 -1.560 0.510 -4.690	6.5	6.1	6.1	$6.47e+25$	322/39/-73	121/53/-104
060776A Luzon	Expo=25 -0.930 5.570 -4.630 -1.810 2.820 -5.740	6.5	6.1	6.4	8.35e+25	249/67/180	339/90/23
081676B Mindanao	Expo=27 9.330 0.240 -9.570 1.450 -3.340 4.330	8.0	6.4	7.9	1.09e+28	341/35/92	158/55/-89
081776A Leyte Philippines	Expo=25 -1.250 0.390 0.860 -0.500 0.070 -0.570	6.0	6.0	5.7	1.34e+25	340/39/67	131/55/-108
081776B Mindanao	Expo=26 -1.220 5.310 -4.100 -1.920 1.330 2.110	7.1	6.2	6.8	5.71e+26	214/64/-172	120/83/-26
081776B Mindanao	Expo=24 -4.620 2.220 2.400 -0.530 -1.810 1.870	5.7	6.0	5.4	4.78e+24	232/35/-76	34/56/-100
110776B Mindanao	Expo=26 1.540 0.230 -1.770 0.990 0.610 -0.170	6.8	6.0	6.8	2.03e+26	162/39/49	30/62/118
112276A Mindanao	Expo=23 2.030 4.260 -6.290 1.780 2.020 0.220	5.1	6.0	0.0	6.07e+23	136/59/14	38/78/148
121476A Ryukyu Isl	Expo=25 -4.160 2.940 1.230 -2.490 0.330 1.350	6.4	6.3	6.2	4.62e+25	230/33/-114	78/61/-75
010177C Honshu Japan	Expo=24 -0.324 0.799 -0.475 1.014 -0.356 0.401	5.4	5.2	0.0	1.34e+24	33/32/-163	289/81/-59
010777B Taiwan Region	Expo=24 -3.009 -0.044 3.054 1.185 -2.128 -0.023	5.7	5.7	5.1	3.88e+24	194/29/-62	343/65/-105
010877A Luzon Philippines	Expo=23 6.364 2.443 -8.807 1.626 -1.176 2.219	5.2	5.3	0.0	8.16e+23	8/43/118	152/53/67
011577A Philippine Isl Reg	Expo=24 -1.842 1.248 0.594 -0.737 0.570 -1.652	5.5	5.6	4.6	2.41e+24	311/34/-88	128/56/-91
011777A Bonin Isl Reg	Expo=24 4.813 0.539 -5.352 0.757 4.521 0.467	5.8	5.6	5.6	6.87e+24	164/25/71	5/66/99
011977B Mindanao	Expo=25 1.646 -0.866 -0.781 -0.990 0.267 1.834	6.2	5.8	5.9	2.45e+25	161/40/130	293/61/62
012077A Mindanao	Expo=24 0.044 1.453 -1.496 0.517 0.947 1.691	5.5	5.4	4.9	2.49e+24	111/65/3	20/87/155
022777A Mariana Islands	Expo=24 -1.502 -0.378 1.880 -0.671 -0.473 -0.742	5.5	5.0	0.0	2.04e+24	136/48/-132	10/56/-53
022877B Mindanao	Expo=24 2.750 -1.458 -1.292 0.444 -0.274 0.678	5.5	5.7	0.0	2.46e+24	313/39/92	130/51/88
030277B Mindanao	Expo=25 3.195 -3.570 0.375 0.728 -1.526 2.261	6.4	6.1	6.1	4.34e+25	271/41/53	135/58/117

*Moment magnitude (Mw); ** Body wave magnitude (Mb); ***Surface wave magnitude (Ms); ****SM: Scalar Moment; *****Fault Plane (FP); ******strike/dip/slip.

Moment magnitude (MW) relies on an underlying robust physical and mathematical development through converting seismic moment using a formula calibrated to agree with MS over much of its range. Others parameters are taken as default ones.

Data are collected in both GMT 'psvelomeca' and GMT 'psmeca' input formats and tested. Final solution was for GMT 'psmeca' (the reason is for the GMT version 5.4.5 compatibility). The focal mechanisms are derived from a solution of the earthquakes' moment tensor, which is estimated by an analysis of the observed seismic waveforms.

Technically, seismic moment tensor (Harvard CMT, with zero trace) was plotted (Fig. 2) by 'psmeca' module using the following GMT code snippet: gmt psmeca -R CMT.txt -J -Sd0.5/8/u -Gred -L0.1p -Fa/5p/it -Fepurple -Fgmagenta -Ft -W0.1p -Fz -Ewhite -O -K >> ps

The scale (0.5) was adjusted to the scaling of the 'beach ball' radius, which is proportional to the magnitude. Here the '-Sd0.5/8/u' implies the scale, label size and annotation placement below the 'beach ball'. Filling of the extensive quadrants was defined by -E parameter; -L parameter defines drawing the 'beach ball' outline of 0.1 pt. Shaded compressional quadrants of the focal mechanism 'beach ball' are colored by -Gred function. The -Fa/5p/it option was used to plot size, P_axis_symbol and T_axis_symbol, to compute and plot P and T axes with symbols (here: selected inverse triangle (i) and triangle (t), respectively).

Focal mechanisms (Figure 2) visualized as commonly accepted in geophysical mapping 'beachballs' show a representation of the lower half of the focal sphere as viewed from above the focus at the earthquake epicenter and respective zones of compression and dilatation. Based on the recorded P-waves dataset, a graphical model shows red areas of the 'beachballs' as upward moving, i.e. compressional motion, while white areas – a downward, dilatational motion. Determining geological information, such as rupture of the Earth's surface, it depicts two nodal planes, fault and auxiliary ones. For instance, auxiliary plane intersects the line of fault plane between the circle and its center of the 'beachball' with the general rule that the closer the intersection is to the center, the more dominant is the strike slip. Increase of the curvature of the crossing hemispheres denotes shallower dip.

The strike of a nodal plane is measured in degrees around the circle from north to the line of the nodal plane. Based on existing classification (Müller, 2001), various focal plane solutions are shown as follows:

1. normal fault striking north, dipping E/W at ca. 45°
2. oblique fault, right or left lateral and reverse slip
3. oblique fault, reverse slip dominant, with some right/left lateral
4. oblique fault, strike slip dominant, attitude ca. N° 40W/70° W (right/left lateral), or N35° E / 70° E (left/right lateral)

The geoid model was plotted based on EGM-2008 grid at PSB margins using geophysical data by Pavlis et al. (2008) and visualized in GMT, Figure 3. The earthquakes event map at PSB area (Figure 5) shows prime hypocentres

and magnitude values by color and size of the circles, respectively. The map was plotted on the basis of International Seismological Centre (ISC-EHB) Bulletin and overplayed on the Google Earth map as a file in Keyhole Markup language Zipped (KMZ), which is a file extension for a placemark file used by Google Earth. The geographic coordinates include x, y, z components in decimal degree defined by the WGS84. The overlay is plotted on Figure 5.

2.2. Velocity mapping

Velocity ellipses with 95% confidence in rotated convention (red) and in (N, E) convention (green), on a PSB region were plotted using 'psvelo' module of GMT (Wessel & Smith, 1998). Theoretical background of the best-fitting angular velocities and Mid-Ocean Ridge VELocity (MORVEL) is presented by DeMets *et al.* (2010) who described and modeled geologically current motions of 25 tectonic plates using geologically determined and geodetically constrained subsets of the global circuit. The datasets include Pacific VELocity (PVEL) (Sella et al. 2002). Technical visualization of the velocity map (Figure 4) was performed using following GMT} code snippet:

- Velocity ellipses in (N,E) convention: 'gmt psvelo CMT.txt -R -J -W0.3p,green -L -Ggreen -Se0.1/0.95/5 -A0.2p -O -K >> ps'. Here, the Vscale gives the scaling of the velocity in inches; the CMT.txt is the dataset; parameters -R and -J indicate the region (in this case coordinates: -R120/152/4/35)
- Velocity ellipses in rotated convention: 'gmt psvelo CMT.txt -R -J -W0.3p,red -Sr0.1/0.95/5 -Ggreen -A0.2p -O -K >> ps'. Here the 'Sr0.1/0.95/5' is the main kwargs showing the Vscale (0.1 inch), Confidence (0.95) and Fontsize (5pt).
- Rotational wedges: 'gmt psvelo CMT.txt -R -J -W0.05p -L -Sw0.5/1.e7 -D2 -Gslateblue2 -Elightgray -A0.2p -O -K >> ps'. Here, the '-Sw0.5/1.e7' indicates Rotational wedges with kwargs as Wedge_scale and Wedge_mag. The '-D2' parameter enables to rescale the uncertainties of velocities by sigma_scale (in this case 2 scale was set up).

The respective red and green circles with confidence ellipses are PVEL dataset estimates, which use a plate circuit to estimate subduction across the plate subduction zones in the west Pacific. According to DeMets *et al.* (1990), relative to the Philippine Sea plate, the Pacific plate rotates counter-clockwise around a pole near the southern end of the plate boundary. The best-fitting angular velocity indicates rapid decrease of the convergence rates southward, from 49\pm 0.7 mm yr-1 (1\sigma) at the northern end of the Izu-Bonin trench to 9\pm 0.8 mm yr-1 of orthogonal subduction along the southern Yap trench, south off Mariana Trench (DeMets et al., 2010).

The PSP-Pacific plate velocities are estimated to fit the interval 1 mm yr-1 and 2° along the lithospheric plate boundary (Sella *et al.,* 2002), which reflects the overlap in the GPS stations used to estimate the motions of the two plates. The existence of the Caroline plate was first proposed by Weissel & Anderson (1978),

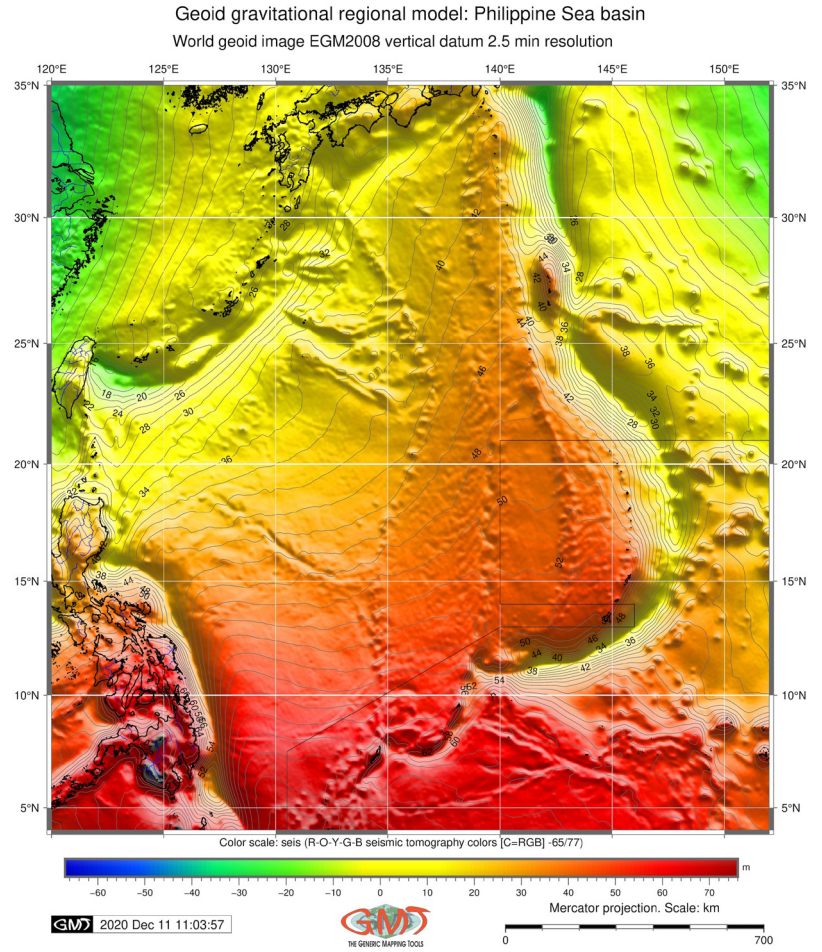

Figure 3. Geoid model based on EGM-2008 grid at PSB margins. Data: Pavlis et al. 2008. Mapping: GMT. Source: author.

who estimated its motions from a synthesis of marine seismic, bathymetric, and seismologic observations from its boundaries with the Pacific and Philippine plates. Located in the western equatorial Pacific immediately south of the PSP (Figure 1), it remains the poorly understood and enigmatic with uncertainties about the style and rate of its present deformation caused by scarcity of reliable kinematic data.

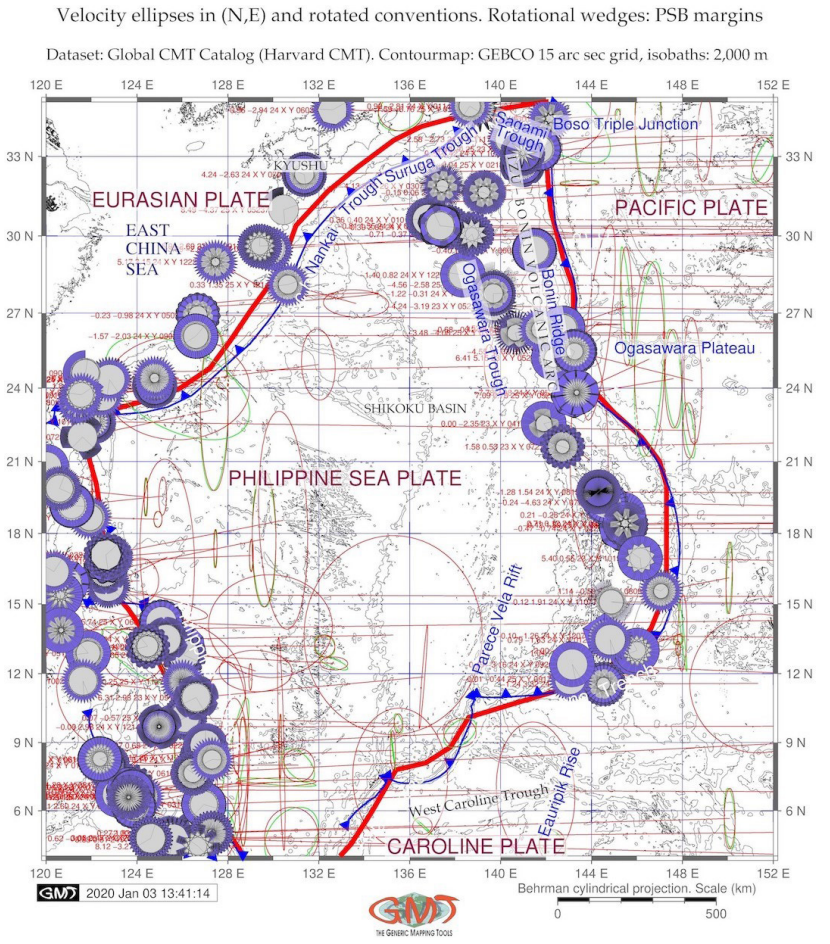

Figure 4. Velocity ellipses at PSB margins from 1976 to 2010 in (N, E) convention (green) and rotated convention (red). Rotational wedges (purple 'gear wheels'): by 'psvelo' module of GMT. Data: Global Centroid-Moment-Tensor (CMT) Project. Contour: GEBCO grid.
Source: author.

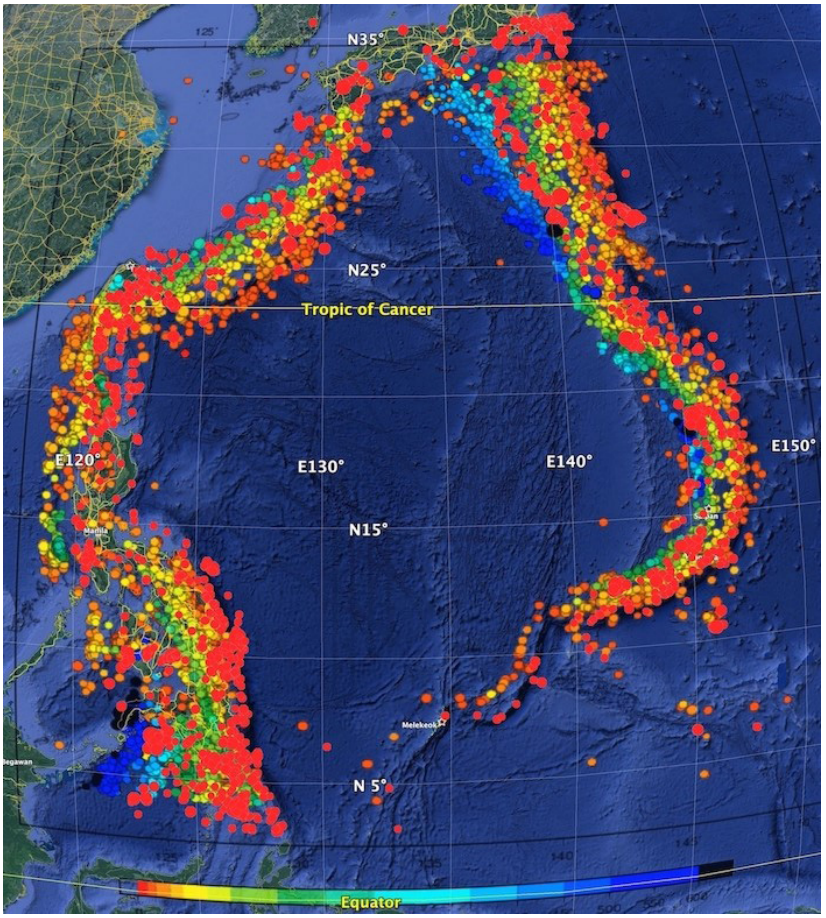

Figure 5. Earthquakes event map at PSB area: prime hypocentres and magnitude values. Data source: http://www.isc.ac.uk/isc-ehb/search/catalogue/ ISC-EHB Bulletin. Circle size shows magnitude values. Circle color shows hypocenter depths, km (from red: 0 to dark blue/black: >600). Cartographic overlay of .kmz data: Google Earth Pro.
Source: author.

3. Results

Seismic phenomena is the PSB (Figure 2) can be explained as the result of tectonic processes at the edges of the lithospheric plates that spread apart at the ocean ridges along the large strike-slip faults and converge at the hot and weak volcanic island arcs of IBM and the Philippines. Seismicity map (Figure 2) in the PSB area shows that most earthquakes are confined to the marginal areas presenting a narrow, continuous belts around large stable areas of the PSP. The activity differs

by divergence and convergence zones being moderate in the zones of plate divergence and including deep shocks at shallow depths in the zones of plate convergence. Seismic data on focal mechanisms are presented at CMT catalogue which gives a relative direction of tectonic plates motion throughout active belts. Focal mechanisms point at relative motions of the lithosphere plates determined from magnetic and topographic data associated with the zones of plate divergence.

A phenomena of the deep-sea trench includes its migration that depends primarily on the age at the trench (Faccenna et al. 2009; Gutscher *et al.*, 2016): located on the place of the subduction plate boundary at a given time, the trench may change its location over time as a result of the complex processes of the global plate tectonics. As proved by Lallemand *et al.* (2008), trench migration and hence, geomorphic fluctuations, depends on the lower plate parameters and controlled by the subducting plate velocity Vsub.

Philippine Sea Basin is marked by the complex interaction of three lithospheric plates: Eurasian, Australian and the PSP, which includes collision, subduction and accretion. Old, heavy and large (103,300,000 km^2) Pacific plate plays the major role comparing to the Australian Plate (47,000,000 km^2) and the PSP 5,500,000 km^2 (Alden, 2019). The morphology of the Pacific plate has a low dip angle at shallow depths. The PSP, a large and tectonically complex region of the western Pacific located between the Pacific, Eurasian and Australian plates, is the world's largest marginal basin plate (Sdrolias *et al.*, 2004). The PSP has two back-arc basins formed in Oligocene to Miocene period: Parece Vela and Shikoku Basins (Figure 1).

Slab dynamics is one of the important driving forces for the trench formation affecting the mechanisms of its migration (retreat or advance). It is therefore crucial to characterize the origin of the subducting slab morphology in the deep mantle identifying the features of subduction zones, which are among the fundamental issues of solid Earth (Yoshida, 2017). Effects of slab mineralogy and phase chemistry on the subduction dynamics (buoyancy, stress field), kinematics (rate of subduction and plate motion), elasticity (deformation and seismic wave speed), thermometry (effects of latent heat, isobaric superheating) and seismicity (adiabatic shear instabilities) are discussed previously (Bina *et al.*, 2001).

4. Conclusion

The datasets were combined with multi-source grids explained in detailed. A multi-source dataset applied in this research includes a compilation of GEBCO, ETOPO1, ETOPO5, CMT, EGM96, GVP and Global Self-consistent Hierarchical High-resolution Geography Database (GSHHGD) sources. Combined studies of seismic and tectonic settings (focal mechanism, velocity, geological lineaments), volcanic activity and general topography of the ocean seafloor are essential for understanding the complicated bathymetry and geomorphic patterns of the trenches in the Philippine Sea Basin. In this paper, a multi-source GIS data analyze on the southern side of the Philippine Sea Basin and discussion of the current situation and historical evolution of the geology of this area was performed and presented.

Research novelty of the presented research consists in the multi-source data analysis applied for geophysical analysis of the current situation representing seismicity of the region, and earthquake locations, magnitude and distribution by intensity via the GMT modules. A combination of the geophysical visualization, geological analysis and GMT based mapping of the Philippine Sea margins does not present in the existing literature. Practical novelty of the work consists in the tested methodology of the GMT-based geophysical data visualization. In contrast to the classic cartographic approaches having GUI, e.g. ArcGIS ESRI based, in geodata visualization and mapping (Gauger *et al.*, 2007; Gohl *et al.*, 2006a, 2006b; Lemenkova, 2011; Kuhn *et al.*, 2006; Suetova *et al.*, 2005a, 2005b; Klaučo *et al.*, 2017, 2013; Lemenkova *et al.*, 2012), or statistical approaches (Lemenkova, 2019e, 2019f), GMT is notable for its scripting algorithms as a core conceptual methodology.

Semi-automated methods of cartographic digitizing presented previously (Schenke & Lemenkova, 2008) was driven by the developed algorithms of the machine learning (ML). Application of the scripting in the cartographic routine, minimizes handmade routine and subjectivity in mapping and increases overall precision of the data processing and visualization accuracy. GMT proposes more advanced solution in the automatization through ML based mapping that results in a high quality cartographic mapping (Lemenkova, 2020a, 2020b, 2020c, 2020d, 2020e). Specifically, among other modules, 'psmeca', 'psvelo' were tested in the current work for seismic mapping and plotting earthquakes focal mechanisms as demonstrated in this paper.

Acknowledgments

This research was implemented into the framework of the project No. 0144-2019-0011, Schmidt Institute of Physics of the Earth, Russian Academy of Sciences. I thank the anonymous reviewers for their comments and suggestions on the initial version of the text.

References

Alden, A. 2019. Here are the Sizes of Tectonic or Lithospheric Plates. https://www.thoughtco.com/sizes-of-tectonic-or-lithospheric-plates-4090143

Bina, C. R.; Stein, S.; Marton, F. C. & Van Ark, E. M. 2001. Implications of slab mineralogy for subduction dynamics. *Physics of the Earth and Planetary Interiors*, 127, 51-66. https://doi.org/10.1016/S0031-9201(01)00221-7

Cao, L.; Wang, Z.; Wu, S. & Gao, X. 2014. A new model of slab tear of the subducting Philippine Sea Plate associated with Kyushu-Palau Ridge subduction. *Tectonophysics*, 636, 158-169. https://doi.org/10.1016/j.tecto.2014.08.012

Chang, W. Y.; Yu, G. K.; Hwang, R. D. & Chiu, J. K. 2007. Lateral Variations of Rayleigh-wave Dispersions in the Philippine Sea region, *Terrestrial, Atmospheric and Oceanic Sciences*, 18, 859-878. https://doi.org/10.3319/TAO.2007.18.5.859(T)

Cížková, H. & Bina, C. R. 2015. Geodynamics of trench advance: Insights from a Philippine-Sea-style geometry. *Earth and Planetary Science Letters*, 430, 408-415. https://doi.org/10.1016/j.epsl.2015.07.004

DeMets, C.; Gordon, R. G.; Argus, D. F. & Stein, S. 1990. Current plate motions. *Geophysical Journal International*, 101, 425-478. https://doi.org/10.1111/j.1365-246X.1990.tb06579.x

DeMets, C.; Gordon, R. G. & Argus, D. F. 2010. Geologically current plate motions. *Geophysical Journal International*, 181, 1-80. https://doi.org/10.1111/j.1365-246X.2009.04491.x

Ekström, G.; Nettles, M. & Dziewonski, A. M. 2012. The global CMT project 2004-2010: Centroid-moment tensors for 13,017 earthquakes. *Physics of the Earth and Planetary Interiors*, 200-201, 1-9. https://doi.org/10.1016/j.pepi.2012.04.002

Faccenna, C.; Giuseppe, E. D.; Funiciello, F.; Lallemand, S. & van Hunen, J. 2009. Control of seafloor aging on the migration of the Izu-Bonin-Mariana Trench. *Earth and Planetary Science Letters*, 288, 386-398. https://doi.org/10.1016/j.epsl.2009.09.042

Fujioka, K.; Okino, K.; Kanamatsu, T.; Ohara, Y.; Ishizuka, O.; Haraguchi, S. & Ishii, T. 1999. Enigmatic extinct spreading center in the West Philippine backarc basin unveiled. *Geology*, 27, 1135-1138. https://doi.org/10.1130/0091-7613(1999)027<1135:EESCIT>2.3.CO;2

Fujioka, K.; Okino, K.; Kanamatsu, T. & Ohara, Y., 2002. Morphology and origin of the Challenger Deep in the Southern Mariana Trench. *Geophysical Research Letters*, 29, 13-72. https://doi.org/10.1029/2001GL013595

Gauger, S.; Kuhn, G.; Gohl, K.; Feigl, T.; Lemenkova, P. & Hillenbrand, C. 2007. Swath-bathymetric mapping. ANT-XXIII/4 R/V 'Polarstern', *Reports on Polar and Marine Research*, 557, 38-45. https://doi.org/10.6084/m9.figshare.7439231

Gohl, K.; Eagles, G.; Udintsev, G.; Larter, R. D.; Uenzelmann-Neben, G.; Schenke, H.-W.; Lemenkova, P.; Grobys, J.; Parsiegla, N.; Schlueter, P.; Deen. T.; Kuhn, G. & Hillenbrand, C.-D. 2006a. Tectonic and sedimentary processes of the West Antarctic margin of the Amundsen Sea embayment and PineIsland Bay. 2nd SCAR Open Science Meeting, 12-14 Jul, Hobart, Australia. https://doi.org/10.6084/m9.figshare.7435484

Gohl, K.; Uenzelmann-Neben, G.; Eagles, G.; Fahl, A.; Feigl, T.; Grobys, J.; Just, J.; Leinweber, V.; Lensch, N.; Mayr, C.; Parsiegla, N.; Rackebrandt, N.; Schlüter, P.; Suckro, S.; Zimmermann, K.; Gauger, S.; Bohlmann, H.; Netzeband, G. & Lemenkova, P., 2006b. "Crustal and Sedimentary Structures and Geodynamic Evolution of the West Antarctic Continental Margin and Pine Island Bay", Expeditionsprogramm Nr.75 ANT XXIII/4 ANT XXIII/5, 11–12. https://doi.org/10.13140/RG.2.2.16473.36961

Gong, W.; Jiang, X.; Guo, Y.; Xing, J.; Li, C. & Sun, Y. 2017. Strike-slip tectonics within the northernmost Philippine Sea plate in an arc continent collisional setting. *Journal of Asian Earth Sciences*, 146, 265-278. https://doi.org/10.1016/j.jseaes.2017.05.032

Gutscher, M. A.; Klingelhoefer, F.; Theunissen, T.; Spakman, W.; Berthet, T.; Wang, T. K. & Lee, C. S. 2016. Thermal modeling of the SW Ryukyu forearc (Taiwan): Implications for the seismogenic zone and the age of the subducting Philippine Sea Plate (Huatung Basin). *Tectonophysics*, 692, 131-142. https://doi.org/10.1016/j.tecto.2016.03.029

Hall, R.; Ali, J.R .; Anderson, C. D. & Baker, S. J. 1995a. Origin and motion history of the Philippine Sea Plate. *Tectonophysics*, 251, 229-250. https://doi.org/10.1016/0040-1951(95)00038-0

Hall, R.; Fuller, M.; Ali, J.R. & Anderson, C. D. 1995b. The Philippine Sea Plate: magnetism and reconstructions. *Geophysical Monograph Series AGU, Active Margins and Marginal Basins of the Western Pacific*, 88, 371-404. https://doi.org/10.1029/GM088p0371

Klaučo, M.; Gregorová, B.; Stankov, U.; Marković, V. & Lemenkova, P. 2017. Land planning as a support for sustainable development based on tourism: A case study of Slovak Rural Region. *Environmental Engineering and Management Journal*, 2 (16), 449-458. https://doi.org/10.30638/eemj.2017.045

Klaučo, M.; Gregorová, B.; Stankov, U.; Marković, V. & Lemenkova, P. 2013. Determination of ecological significance based on geostatistical assessment: a case study from the Slovak Natura 2000 protected area. *Central European Journal of Geosciences*, 5 (1), 28-42. https://doi.org/10.2478/s13533-012-0120-0

Kuhn, G.; Hass, C.; Kober, M.; Petitat, M.; Feigl, T.; Hillenbrand, C. D.; Kruger, S.; Forwick, M.; Gauger, S. & Lemenkova, P. 2006. The response of quaternary climatic cycles in the south-east pacific: development of the opal belt and dynamics behavior of the west antarctic ice sheet. Expeditions programm Nr. 75 ANT XXIII/4, AWI, Bremerhaven, Germany. https://doi.org/10.13140/RG.2.2.11468.87687

Lallemand, S.; Heuret, A.; Faccenna, C. & Funiciello F. 2008. Subduction dynamics as revealed by trench migration. *Tectonics*, 27: TC3014. https://doi.org/10.1029/2007TC002212

Lemenkova, P.; Promper, C. & Glade, T., 2012. Economic Assessment of Landslide Risk for the Waidhofen a.d. Ybbs Region, Alpine Foreland, Lower Austria. Protecting Society through Improved Understanding. 11th International Symposium on Landslides & the 2nd North American Symposium on Landslides & Engineered Slopes (NASL), June 2-8, 2012. Canada, Banff, 279-285. https://doi.org/10.6084/m9.figshare.7434230

Lemenkova, P. 2011. *Seagrass Mapping and Monitoring Along the Coasts of Crete, Greece*, M.Sc. Thesis. https://doi.org/10.13140/RG.2.2.16945.22881

Lemenkova, P. 2018. R scripting libraries for comparative analysis of the correlation methods to identify factors affecting Mariana Trench formation. *Journal of Marine Technology and Environment*, 2, 35-42. https://doi.org/10.6084/m9.figshare.7434167

Lemenkova, P. 2019a. GMT Based Comparative Analysis and Geomorphological Mapping of the Kermadec and Tonga Trenches, Southwest Pacific Ocean. *Geographia Technica*, 14 (2), 39-48. https://doi.org/10.21163/GT_2019.142.04

Lemenkova, P. 2019b. Statistical Analysis of the Mariana Trench Geomorphology Using R Programming Language. *Geodesy and Cartography*, 45 (2), 57-84. https://doi.org/10.3846/gac.2019.3785

Lemenkova, P. 2019c. Geomorphological modelling and mapping of the Peru-Chile Trench by GMT. *Polish Cartographical Review*, 51 (4), 181-194. https://doi.org/10.2478/pcr-2019-0015

Lemenkova, P. 2019d. Geospatial Analysis by Python and R: Geomorphology of the Philippine Trench, Pacific Ocean. *Electronic Letters on Science and Engineering*, 15 (3), 81-94. https://doi.org/10.6084/m9.figshare.11449362

Lemenkova, P. 2019e. Geophysical Modelling of the Middle America Trench using GMT. *Annals of Valahia University of Targoviste. Geographical Series*, 19 (2), 73-94. https://doi.org/10.6084/m9.figshare.12005148

Lemenkova, P. 2019f. AWK and GNU Octave Programming Languages Integrated with Generic Mapping Tools for Geomorphological Analysis. *GeoScience Engineering*, 65 (4), 1-22. https://doi.org/10.35180/gse-2019-0020

Lemenkova, P. 2020a. Variations in the bathymetry and bottom morphology of the Izu-Bonin Trench modelled by GMT. *Bulletin of Geography. Physical Geography Series*, 18 (1), 41-60. https://doi.org/10.2478/bgeo-2020-0004

Lemenkova, P. 2020b. GEBCO Gridded Bathymetric Datasets for Mapping Japan Trench Geomorphology by Means of GMT Scripting Toolset. *Geodesy and Cartography,* 46 (3), 98-112. https://doi.org/10.3846/gac.2020.11524

Lemenkova, P. 2020c. Geomorphology of the Puerto Rico Trench and Cayman Trough in the Context of the Geological Evolution of the Caribbean Sea. *Annales Universitatis Mariae Curie-Sklodowska, sectio B – Geographia, Geologia, Mineralogia et Petrographia*, 75, 115-141. https://doi.org/10.17951/b.2020.75.115-141

Lemenkova, P. 2020d. The geomorphology of the Makran Trench in the context of the geological and geophysical settings of the Arabian Sea. *Geology, Geophysics and Environment*, 46 (3), 205-222. https://doi.org/10.7494/geol.2020.46.3.205

Lemenkova, P. 2020e. Using GMT for 2D and 3D Modeling of the Ryukyu Trench Topography, Pacific Ocean. *Miscellanea Geographica*, 25 (3), 1-13. https://doi.org/10.2478/mgrsd-2020-0038

Lemenkova, P. 2020f. NOAA Marine Geophysical Data and a GEBCO Grid for the Topographical Analysis of Japanese Archipelago by Means of GRASS GIS and GDAL Library. *Geomatics and Environmental Engineering*, 14 (4), 25-45. https://doi.org/10.7494/geom.2020.14.4.25

Lin, J. Y. & Lo, C. L. 2013. Earthquake-induced crustal gravitational potential energy change in the Philippine area. *Journal of Asian Earth Sciences*, 66, 215-223. https://doi.org/10.1016/j.jseaes.2013.01.009

Menard, H. W., 1955. Deep-sea channels, topography, and sedimentation. *American Association of Petroleum Geologists Bulletin*, 39, 236-255.

Müller, D., 2001. Deep Earth Structure and Global Tectonics. University of Sydney, School of Geosciences, Division of Geology and Geophysics, GEOL Geological Hazards and Solutions.

Ogawa, Y.; Kobayashi, K.; Hotta, H. & Fujioka, K. 1997. Tension cracks on the oceanward slopes of the northern Japan and Mariana Trenches. *Marine Geology*, 141, 111-123. https://doi.org/10.1016/S0025-3227(97)00059-5

Ozawa, A.; Tagami, T.; Listanco, E. L.; Arpa, C. B. & Sudo, M. 2004. Initiation and propagation of subduction along the Philippine Trench: evidence from the temporal and spatial distribution of volcanoes. *Journal of Asian Earth Sciences*, 23, 105-111. https://doi.org/10.1016/S1367-9120(03)00112-3

Pavlis, N. K.; Holmes, S. A.; Kenyon, S. C. & Factor, J. K. 2012. The development and evaluation of the Earth Gravitational Model 2008 (EGM2008). *Journal of Geophysical Research*, 117: B04406. https://doi.org/10.1029/2011JB008916

Samowitz, I. R. & Forsyth, D. W. 1981. Double seismic zone beneath the Mariana Island arc. *Journal of Geophysical Research*, 86, 7013-7021. https://doi.org/10.1029/JB086iB08p07013

Schenke, H. W. & Lemenkova, P. 2008. Zur Frage der Meeresboden-Kartographie: Die Nutzung von AutoTrace Digitizer für die Vektorisierung der Bathymetrischen Daten in der Petschora-See. *Hydrographische Nachrichten*, 25 (81), 16-21. https://doi.org/10.6084/m9.figshare.7435538

Sdrolias, M.; Roest, W. R. & Müller, R. D. 2004. An expression of Philippine Sea plate rotation: the Parece Vela and Shikoku Basins. *Tectonophysics*, 394, 69-86. https://doi.org/10.1016/j.tecto.2004.07.061

Seekings, L. C. & Teng, T. L. 1977. Lateral variations in the structure of the Philippine Sea Plate, *Journal of Geophysical Research*, 82, 317-324. https://doi.org/10.1029/JB082i002p00317

Sella, G. F.; Dixon, T. H. & Mao, A. 2002. REVEL: a model for recent plate velocities from space geodesy. *Journal of Geophysical Research*, 107, 11-30. https://doi.org/10.1029/2000JB000033

Suetova, I.; Ushakova, L. & Lemenkova, P. 2005a. Geoinformation mapping of the Barents and Pechora Seas. *Geography and Natural Resources*, 4, 138-142. https://doi.org/10.6084/m9.figshare.7435535

Suetova, I.; Ushakova, L. & Lemenkova, P. 2005b. Geoecological Mapping of the Barents Sea Using GIS. *International Cartographic Conference*. July 9–16, La Coruna, Spain. https://doi.org/10.6084/m9.figshare.7435529

Weissel, J. K. & Anderson, R. N. 1978. Is there a Caroline plate? *Earth Planetary Science Letters*, 41, 143-158. https://doi.org/10.1016/0012-821X(78)90004-3

Wessel, P. & Smith, W. H. F. 1998. New, improved version of generic mapping tools released, *EOS Transactions of the AGU*, 79 (47), 579-579. https://doi.org/10.1029/98EO00426

Yoshida, M. 2017. Trench dynamics: Effects of dynamically migrating trench on subducting slab morphology and characteristics of subduction zones systems. *Physics of the Earth and Planetary Interiors*, 268, 35-53. https://doi.org/10.1016/j.pepi.2017.05.004